

# Uncertainty in the Absolute Calibration of Radar Differential Radar Reflectivity

Earle R. Williams, Kenta T. Hood, David J. Smalley, Michael F. Donovan, Betty J. Bennett and E. Griffin

Massachusetts Institute of Technology, Lincoln Laboratory

## 1. INTRODUCTION

In the calibration of any measurement, one seeks a standard that is substantially better known than any quantity one would hope to measure. The challenge set forth in achieving 0.1 dB uncertainty in radar differential reflectivity (ZDR) (Zrnic et al., 2006) is appropriate in this context. This stringent criterion amounts to a difference of 2.3% between the reflectivity at horizontal and vertical polarization, and is subsequently referred to as the ‘Holy Grail’. The suggested real-time monitoring of the calibration of ZDR in light rain and snow does not meet this standard because the intrinsic values of such precipitation targets are not well known at this level of uncertainty. Accordingly, these methods have been referred to as ‘pseudo-calibration’ (Williams et al., 2013). Drizzle (raindrops <500  $\mu\text{m}$  in diameter) is a suitable calibration target for ZDR, but unfortunately its isolated presence is often difficult to verify.

The availability of dual-pol capability at 150 NEXRAD radars over the United States has motivated the development of reliable calibration methods for differential reflectivity (ZDR). The traditional vertically-pointing, or ‘bird bath’, offset check (Bringi and Chandrasekar, 2005) is unfortunately not practical with contemporary NEXRAD antenna design. The current assessment for the US network shows the majority of NEXRAD radars to be out of

calibration by the 0.1 dB standard (Cunningham et al., 2013). These results stand in contrast with the radar network operated by the German Wetterdienst (Frech, 2015), whose success in this regard is attributable to calibration by vertically pointing.

Calibration methods other than vertically pointing must be considered and evaluated for NEXRAD. Three methods are considered here: the use of Bragg scatter (Melnikov et al. 2013), the use of natural microwave emission from the Sun (Holleman et al., 2010; Gabella et al., 2015), and the use of a metal sphere (standard target). A fourth method known as “cross pol” (Hubbert et al., 2003) was not studied here for lack of available data. It will be shown here that even when calibration methods with known values of mean ZDR = 0 are used, substantial variability is manifest in the measurements.

## 2. BRAGG SCATTER

The speed of light in vacuum is modified in air by the subtle variations in dielectric permittivity caused by the presence of matter. Water vapor is the dominant contributor in cloud-free conditions because of the strongly polarizable water molecule. The turbulent atmosphere is characterized by fluctuations in temperature and humidity, and thereby in refractive index, over a wide range of scales. Both observations and theory show that this homogeneous, isotropic turbulence follows predictable power law behavior (Kolmogorov, 1962). The selective backscatter of radar waves from this random medium at a specific scale equaling half a radar wavelength (for purposes of constructive interference in the radar return), was worked out mathematically by Tatarski (1961). The mechanism is now commonly called Bragg scatter (Gossard and Strauch,

---

This work was sponsored by the Federal Aviation Administration under Air Force Contract FA8721-05-C-0002. Opinions, interpretations, conclusions, and recommendations are those of the authors and are not necessarily endorsed by the U.S. Government.

*Corresponding author address:* Earle Williams, MIT Lincoln Laboratory, 244 Wood St., Lexington, MA 02420-9185; e-mail: earlew@ll.mit.edu.

1983), by virtue of its similarity to the scattering of X-rays by specific scales between planes in a crystal lattice.

Melnikov (2013) has recently suggested the use of Bragg scatter to calibrate radar differential reflectivity. The physical basis for this idea is that atmospheric turbulence is isotropic, providing for the statistically matched backscatter return of both horizontal (H) and vertical (V) polarizations in dual-pol measurements, with an expected mean ZDR value of 0 dB.

Experimental tests of this suggestion using observations from the KOUN NEXRAD radar are shown in Figure 1. Integration of 128 pulses was undertaken in these measurements to produce these distributions of differential reflectivity. Sample distributions are shown on four separate days, but all exhibit similar features. In conformity with the idea that clear air turbulence is isotropic, the means of the distributions are within a few tenths of dB from zero. More noteworthy from the standpoint of the main topic of this study—uncertainty in calibration—the standard deviation of these measurements is  $\sim 0.4$  dB, well outside the range of the Holy Grail. One should be able to reduce this standard deviation, in keeping with the well known results in statistics, by longer dwell time and larger numbers of independent samples. However, in operational scanning one will have limits imposed on dwell time by the necessary update rate of volume scans.

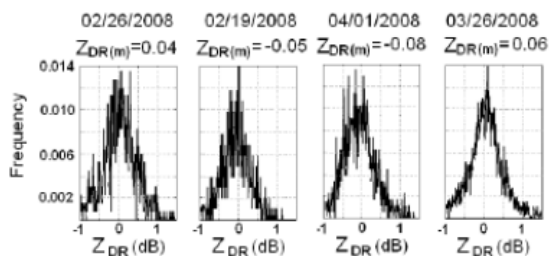


Figure 1 Distributions of differential reflectivity based on sequences with 128 radar samples, on four separate days (February-April, 2008).

The most serious challenge to the use of Bragg scatter for calibration purposes is the ubiquitous presence of insects in the boundary layer in the warm season. Even in dry desert environments, insects are commonplace, particularly at night. These biological targets not only dominate over the relatively weak Bragg scatter in the radar returns, but worse, can present pronounced departures from isotropic scattering. Dragonflies, for example, may exhibit differential reflectivity of several dB. For the foregoing reasons, Bragg calibration would be restricted to winter months when insects are absent. Then one encounters the negative impact of reduced water vapor (and reduced Bragg scatter intensity) due to the Clausius-Clapeyron relationship. The temperature dependence of Bragg backscatter deserves further study.

### 3. THE SUN

The Sun is an ordinary star and like the great majority of stars, exhibits a time-average polarization in the optical range which differs by less than 1% from zero. Stars are less studied in the microwave region, but fortuitously, the Sun has been monitored at S-band for more than half a century (Covington, 1947; Tapping, 2015). A frequency of 2800 MHz (10.7 cm wavelength) was selected as a sensitive monitor of the 11-year solar cycle, now with the realization that this highly non-thermal component of solar radiation is selectively emitted from sunspots. The sunspot origin in strong magnetic fields gave the S-band emission a quantitative advantage over the counting of sunspots, while retaining a large ( $\sim$ factor-of-two) variation over the 11-year solar cycle. (In contrast, the quasi-black-body thermal emission, more uniformly distributed over the solar disc, changes little because the integrated emission changes by only 0.1% over the solar cycle. If that modest change in power were ascribed to a change in effective black body temperature via Stefan's law, that would amount to a temperature change of only a few hundredths of one degree C. In this context, the observed

change in emission at 10.7 cm wavelength is huge.)

The highly concentrated nature of the S-band emission from the Sun in sunspots has been documented in interferometric measurements from Earth, with a resolution of 2.7 to 36.7 seconds of arc (Lang, 1977). This resolution is appropriate as typical sunspot cores are 10-20 arc seconds in diameter, or 7000-14000 km on the solar surface. The physical basis for the S-band emission is gyromagnetic radiation from energetic electrons rotating around the magnetic field lines that are characteristic of sunspots. The formula for electron gyrofrequency  $f$  is:

$$f = \frac{eB}{2\pi m}$$

where  $e$  is the electronic charge,  $m$  is the electronic mass, and  $B$  is the magnitude of the magnetic field. For magnetic field values characteristic of sunspots (several thousand gauss), the electron gyrofrequency is in the microwave region. For a field of 1000 gauss, the gyrofrequency is exactly 2.8 GHz, and that is how the monitoring convention at 10.7 cm came to be. The sunspot microwave emission is dominated by circular polarization (Krueger, 1979; Tapping, 2015), with contributions from right hand circular and left hand circular associated with the two polarities of magnetic field that characterize each sunspot.

The polarimetric measurements on the Sun described here were extracted from a box scan of the Sun carried out with the KOUN dual-pol S-band radar in Norman, Oklahoma. The radar wavelength is 11.08 cm (2706 GHz) and so not very different than the one chosen for solar monitoring by the National Research Council in Canada (Tapping, 2015). The radar elevation angle for these measurements was near 31 degrees, and so ground clutter effects were minimal. The measured SNR in the KOUN receiver channels was approximately 20 dB.

Figure 2 shows the pulse-to-pulse radar differential reflectivity from the Sun. Great variability is evident with maximum values

reaching +/- 20 dB. The mean value looks to be close to zero but on this scale of presentation, that is difficult to discern. One can organize all these time samples into a distribution of pulse-to-pulse values of ZDR and that is shown in Figure 3. The standard deviation of these measurements is quite large at 7.9 dB

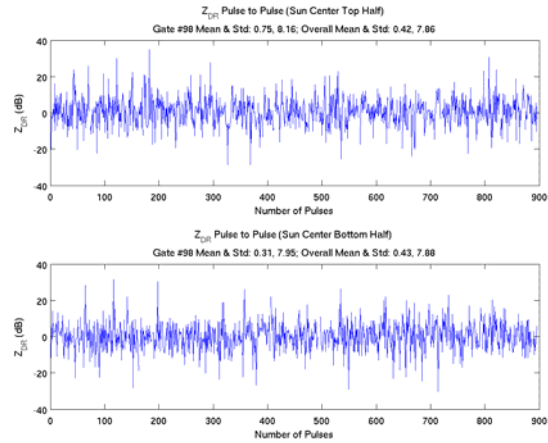


Figure 2 Pulse-to-pulse time series of differential reflectivity ZDR (in dB) from the Sun during slow scanning over the solar disc. Radar sampling rate is 322 Hz. Radar elevation angle is ~31 degrees.

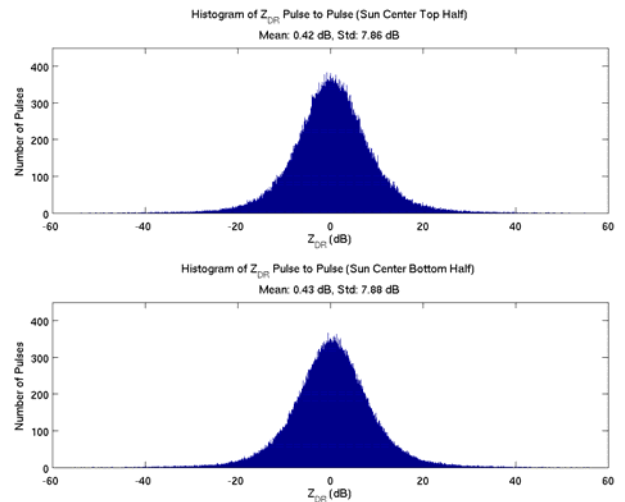


Figure 3 Distribution of pulse-to-pulse values of differential reflectivity ZDR (in dB) obtained over a total sample interval of ~2.8 seconds. The upper (lower) plots represent the upper (lower) portions of the Sun scan. The standard deviation of these measurements is 7.9 dB (half-width 15.8 dB).

Figure 4 shows the ZDR distribution for new samples formed by integrating 128 raw samples, in keeping with the earlier procedure for Bragg scatter. The standard deviation has now diminished to 0.6 dB, but is still large relative to the Holy Grail.

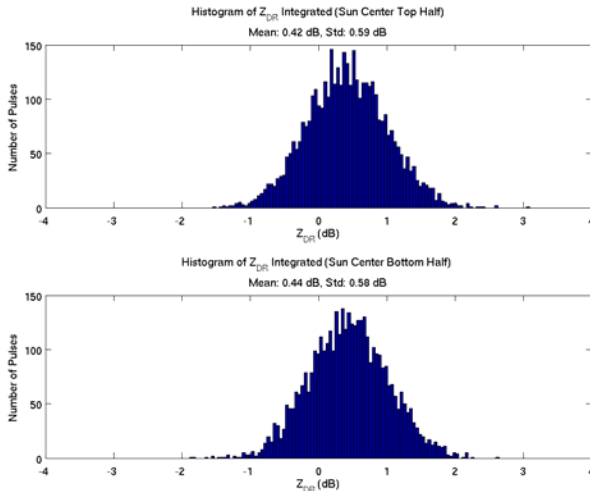


Figure 4 Distribution of values of differential reflectivity ZDR (in dB) based on 128-sample integrations. The upper (lower) plots represent the upper (lower) portions of the Sun scan. The standard deviation of these measurements is 0.6 dB. The distributions are less smooth than the ones in Figure 3 because the total number of values has been reduced by a factor 1/128.

#### 4. METAL SPHERES

Metals spheres have been used for reflectivity calibration on radars for decades (Atlas and Mossop, 1960), but only recently for differential reflectivity (Williams et al., 2013). One particular advantage of the sphere is that it can be used simultaneously to calibrate both reflectivity and differential reflectivity. These calibration checks are also end-to-end in the sense that the entire transmission/reception path (transmitter channels, antenna, sphere, antenna, receiver channels) is checked in the calibration measurement. Furthermore, and of greatest importance to this study, of all the calibration methods ever suggested for differential reflectivity, this one comes closest to the stringent calibration standard discussed in the

Introduction. Commercially available hollow metal spheres have diameters and sphericities known with sufficient accuracy to make their intrinsic radar crosssection and ZDR values less than some hundredths of a dB—far superior to the Holy Grail in the ZDR category.

One major difficulty with the tethered sphere calibration method is the difficulty with the displacements of the sphere and balloon tether by wind. It is particularly important to keep the sphere target centered in the pulse resolution volume of the radar, as illustrated in Figure 5. In the measurements undertaken in Williams et al. (2013) special care was taken to find a period after dark with calm conditions.

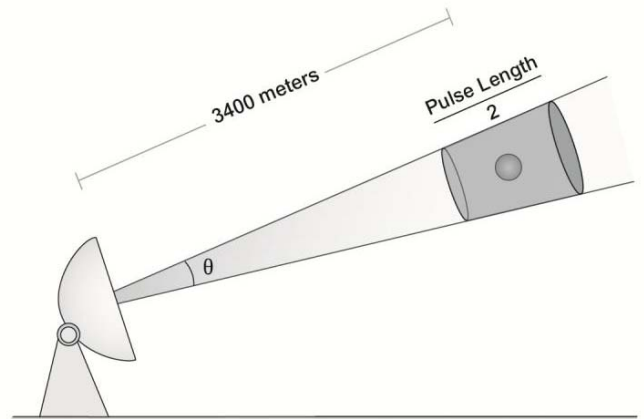


Figure 5 Schematic illustration of calibration sphere centered in the pulse resolution volume of the radar.

Figure 6 shows the time series of pulse-to-pulse samples in differential reflectivity, in dB. Contrary to the initial expectation for a steady zero value of ZDR for a single point target, considerable variability is present, with extreme values reaching +/- 0.5 dB. The computed distribution of ZDR values is shown in Figure 7, and shows a standard deviation of 0.41 dB. In the same vein as the earlier procedure for Bragg scatter and for the Sun samples, we can integrate the pulse-to-pulse observations into 128-point samples. The distribution of these ZDR values is shown in Figure 8. The standard deviation has been reduced, as expected, but

still exceeds the Holy Grail by an uncomfortable margin.

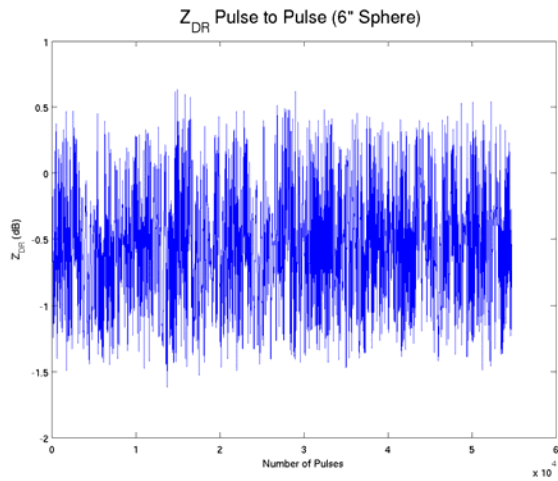


Figure 6 Pulse-to-pulse time series of differential reflectivity on the 6-inch diameter metal sphere from Williams et al. (2013) over a total time interval of ~60 seconds. The radar sampling rate is 322 Hz. The radar elevation angle is ~2.5 degrees.

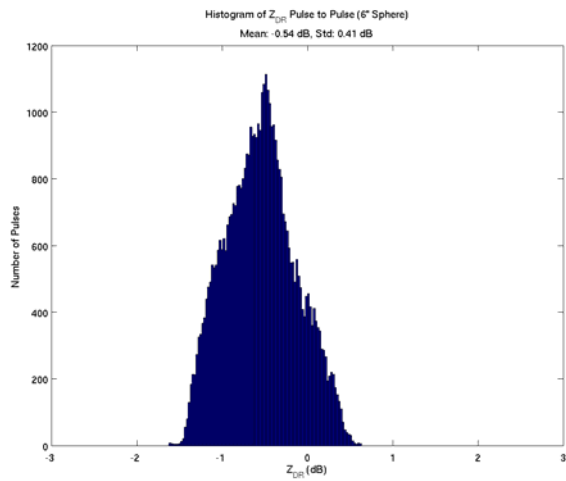


Figure 7 Distribution of pulse-to-pulse values of differential reflectivity ZDR (in dB) for the 6 inch diameter sphere over a period of ~10 seconds.

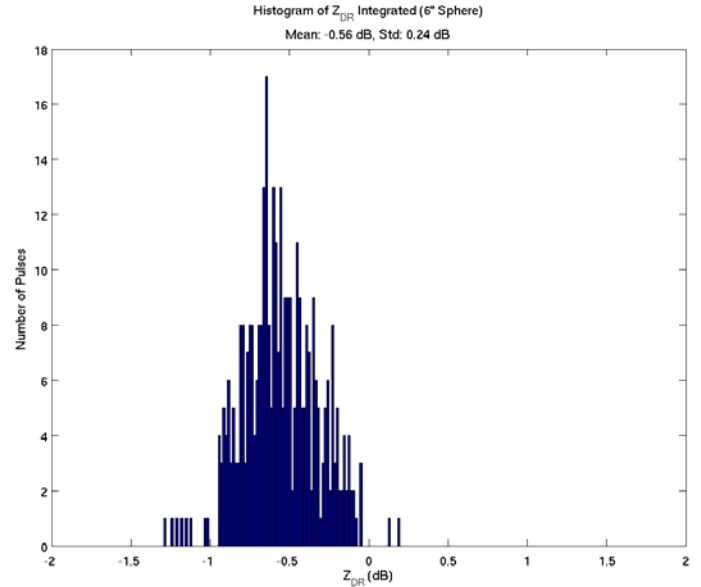


Figure 8 Distribution of values of differential reflectivity ZDR (in dB) based on 128 pulse-to-pulse samples. The standard deviation of these measurements is 0.24 dB. This distribution is less smooth than in Figure 7 because the number of samples has been reduced by a factor 1/128.

## 5. DISCUSSION

Three methods have been considered for the calibration of radar differential reflectivity. All three methods exhibit substantial variability on short time scales that greatly exceeds the Holy Grail criterion of 0.1 dB. Even when 128 sample integrations are considered, the standard deviations from the mean values exceed by many times 0.1 dB. Table 1 summarizes the results.

**Table 1** Summary of results on variability in ZDR calibration

Calibration method	Standard Deviation (Pulse-to-pulse)	Standard Deviation (128-pulse integration)
Bragg scatter	N.A.	0.4 dB
Sun	7.9 dB	0.6 dB
Metal sphere	0.41 dB	0.24 dB

The Bragg scatter medium and the emissions from the Sun represent random media that are inherently variable and represent a superposition of contributions with random phase within the resolution of the radar beam. We had expectations that one could escape this variability with a metal sphere as a point target, well-centered in the pulse resolution volume (Figure 5), but even here considerable variability is experienced. The source of this variability has not been resolved, but the two leading hypotheses are the variability of the Bragg medium, and multipath effects with interference from sidelobe contributions. Studies with ultra-short pulse lasers in the optical range show clear evidence for jitter in arrival times through the Bragg medium, but the impact on ZDR variability remains unclear (Williams et al., 2013). Tatarski (1967) made predictions for depolarization effects in the Bragg medium in the optical range, but calculations at S-band using this theory fall way short of the mark in explaining the observed variability. This conclusion seems broadly consistent with findings in Wheelon (2003). The multipath explanation is favored by the evidence in asymmetry between H and V pulses, with total power correlated with the ZDR fluctuations for the V channel, but not for the H channel, consistent with a stronger sidelobe return in the V channel. But we are currently unable to account for the observed variability in ZDR with either explanation.

## 6. CONCLUSION

The loss of vertically-pointing capability for calibration checking with NEXRAD radars prevents the use of the simplest reliable method, and attention should be given to a work-around this limitation. All the additional calibration methods considered here involve substantial variability, even with sample integration, with standard deviations that exceed the 0.1 dB Holy Grail. The latter aspect can be improved upon if sufficient dwell time is possible. Bragg scatter and metal sphere methods both satisfy end-to-end calibration, but the Bragg method will be limited to insect-free seasons. Calibration with

the Sun, always available at S-band in daytime, serves only the antenna/receiver portion. The sphere calibration is the most difficult and time-consuming to implement, but has compensating benefits: the method that promises the least variability and also serves to calibrate both Z and ZDR. Satisfactory results with multiple calibration methods on the same radar will provide the best overall assurance.

## 7. ACKNOWLEDGEMENTS

Discussion on these topics with M. Frech, J. Hubbert, V. Melnikov, K. Tapping, D. Zittel and D. Znic are much appreciated. S. Dodge provided valuable assistance with the organization of the manuscript.

## 8. REFERENCES

- Atlas, D. and S.C. Mossop, Calibration of a weather radar by using a standard target. *Bull. Am. Met. Soc.*, 41, 377-382, 1960.
- Bringi, V.N. and V. Chandrasekar, 2005: *Polarimetric Doppler Weather Radar: Principles and Applications*, Cambridge University Press.
- Covington, A.E., Micro-wave solar noise observations during the partial eclipse of November 23, 1946, *Nature*, 159, 405, 1947.
- Cunningham, J.G., W.D. Zittel, R.R. Lee, R.L. Ice and N.P. Hoban, Methods for identifying systematic differential reflectivity (ZDR) biases on the operational WSR-88D network, 36<sup>th</sup> Conference on Radar Meteorology, American Meteorological Society, Breckenridge, CO., September, 2013.
- Frech, M., Operational radar networks and products, 36<sup>th</sup> Conference on Radar Meteorology, American Meteorological Society, Norman, Oklahoma, September, 2015.
- Gabella, M., M. Sartori, M. Boscacci and U. Germann, Vertical and horizontal polarization observations of slowly varying solar emissions from operational Swiss weather radars, *Atmosphere*, 6, 50-59, doi:10.3390/atmos6010050, 2015.

Gossard, E.E. and R.G. Strauch, *Radar Observations of Clear air and Clouds*, Elsevier, 1983.

Holleman, I., A. Huuskonen, R. Gill and P. Tabary, Operational monitoring of radar differential reflectivity using the Sun, *J. Atmos. Ocean. Tech.*, 27, 881-887, 2010.

Hubbert, J.C., V.N. Bringi and D. Brunkow, Studies of the Polarimetric Covariance Matrix, Part I: Calibration Methodology, *J Atmos. Oceanic Technol.*, 60, 696-706, 2003.

Kolmogorov, A.N., A refinement of previous hypotheses concerning the local structure of turbulence in a viscous incompressible fluid at high Reynolds number, *J. Fluid Mech.*, 13, 82-85, 1962.

Krueger, A., *Introduction to Solar Radio Astronomy and Radio Physics*, Reidel Publishing, 1979.

Lang, K.R., High resolution polarimetry of the Sun at 3.7 and 11.1 cm wavelengths, *Solar Physics*, 52, 63-68, 1977.

Melnikov, V., D. Zrnic, M. Schmidt, and R. Murnan, ZDR calibration issues in the WSR-88Ds, Report on 2013-MOU, 30 September, 2013.

Tapping, K.F., The 10.7cm solar radio flux ( $F_{10.7}$ ), *Space Weather*, (in press), 2015.

Tatarski, V.I., *Wave propagation in a turbulent medium*, Translated by R.A. Silverman, McGraw-Hill, New York, 285 pp.

Tatarski, V.I., Depolarization of light by turbulent atmospheric inhomogeneities, *Radio Physics and Quantum Electronics*, 10, No. 12, 987-988, 1967.

Wheeler, A.D., *Electromagnetic Scintillation*, Vol. II Weak Scattering, Cambridge University Press, 2003.

Williams, E., K. Hood, D. Smalley, M. Donovan, V. Melnikov, D. Forsyth, D. Zrnic, D. Burgess, M.

Douglas, J. Sandifer, D. Saxion, O. Boydston, A. Heck and T. Webster, End-to-end calibration of NEXRAD differential reflectivity with metal spheres, Conference on Radar Meteorology, American Meteorological Society, Breckenridge, CO., September, 2013.

Zrnić, D.S., V.M. Melnikov and J.K. Carter, Calibrating differential reflectivity on the WSR-88D. *J. Atmos. Ocean. Tech.*, 23, 944-951, 2006.